One-dimensional Cooperative Localization for Vehicles equipped with mono-frequency GNSS receivers

Elwan Héry, Philippe Xu and Philippe Bonnifait
Sorbonne universités, Université de Technologie de Compiègne, CNRS UMR 7253 Heudiasyc
57 Av. Landshut CS 60319, 60203 Compiègne cedex, France
Emails: {elwan.hery - philippe.xu - philippe.bonnifait} @hds.utc.fr

***Abstract*— Localization is an important issue for autonomous vehicle navigation. In this paper, we present a one-dimensional cooperative localization problem by using curvilinear abscissa with respect to a reference map. This is made possible by using a high-definition map containing accurate information, such as lane markings which can be used to reduce significantly the cross-track and heading errors. In the context of cooperative localization, a vehicle can use its perception capabilities along with V2V communication to retrieve the relative pose of another vehicle in order to improve the accuracy of its own pose estimate. Experimental results with non independent data coming from communication devices show the necessity to use a more consistent algorithm for data fusion than the classical Kalman filter, such as covariance intersection. The results presented in this paper also show that the one-dimensional cooperative localization algorithm is particularly useful on curved roads since the accuracy increases when cooperative vehicles drive in such conditions.**

I. Introduction

Localization of vehicles is an important problem for autonomous vehicles navigation, despite numerous works [10], poses estimation, i.e., positions and orientations, with lane-level accuracy remains an important issue for autonomous vehicles driving. These pose estimates must be accurate and consistent in order to be used safely for navigation.

Exteroceptive sensors such as LiDAR or camera are becoming more accurate, these sensors give important perception information about obstacles and other vehicles and can also be used to detect landmarks such as lane markings. These lane markings information coupled with high-definition maps [1], [3] that include the true positions of these lane markings give the possibility to correct the localization significantly [9]. The cross-track and heading errors are the principal parts of this localization accuracy increase. Indeed, on straight roads, lane markings are invariant along the road.

In this paper, we propose a new approach, introduced in [5], to reduce the along-track errors. We suppose that the cross-track and heading errors are well known and use the curvilinear abscissa [4], [8] to represent the state of the vehicle.

This one-dimensional approach uses different methods for data fusion like the classical Kalman filter to compute the curvilinear abscissa of the vehicle. Beside the use of dead-reckoning sensors to know the speed of the vehicle and low cost mono-frequency sensors such as Ublox 8T receiver, the data fusion can use V2V communications to receive the pose estimate of another vehicle and a perception sensor to compute the pose of this second vehicle in the host vehicle frame. The communication can be used to propagate the positioning accuracy of one car to another. It gives the possibility to receive data from the sensors of other cars to improve the estimation of the host vehicle state [7], [12], [15].

The use of data fusion on communicating cars can lead to data incest if one vehicle uses the pose estimate of another vehicle which is itself computed with its own pose. In practice, GNSS errors of two cars driving together are not independent. In these cases, to ensure a consistent localization a covariance intersection filter [6], [11], [15]can be used.

This paper presents also experimental results computed from data recorded with two autonomous Renault Zoé cars equipped with dead-reckoning and exteroceptive sensors for autonomous navigation. These two cars drove together on an experimental road for which a high-definition map was available.

Sec. II introduces the problem of cooperative localization with the experimental platform used to record all the necessary data. In Sec. III, we present the used discretized map. In Sec. IV, we introduce the curvilinear coordinates with continuous and discretized maps. Sec. V, presents the different steps used for the data fusion, the prediction and the updates with the Kalman filter and the covariance intersection filter. Finally, in Sec. VI, experimental results are provided and discussed.

II. Problem statement

Let consider two cars on a road. For the experimental results, we recorded the data of two Renault Zoé cars equipped to do autonomous driving (Fig. 1). For our localization problem, we used a Novatel's Span CPT, an RTK GNSS receiver with an inertial measurement unit, to provide the ground truth of the cars. We used the low cost mono-frequency GNSS receiver Ublox 8T for the localization of the cars. We also used the dead-reckoning sensors already present in the commercialized Renault Zoé. With these sensors, we had access to the wheels speeds directly from the CAN bus of the vehicles. Perception sensors gave us the possibility to localize other vehicles in the local frame of the vehicle using it. To obtain a perfect relative localization, the ground truth

Fig. 1: Experimental Renault Zoé cars.

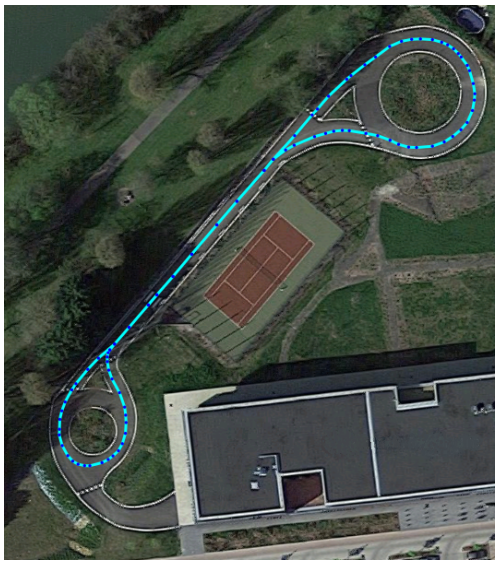

Fig. 2: Experimental road Séville (Google Map).

was used to simulate the perception between both cars. In practice, this local localization could also be done with a LiDAR or a camera. For a one-dimensional problem, we supposed that we had an accurate lateral localization and an accurate heading estimation. In practice, these accurate estimates could be computed using camera and LiDAR along with high-definition maps.

During the reported experiment, the two cars were following each other in the experimental road Seville (Fig.2). The gray car was the leading vehicle and the white car was the following vehicle. This experimentation used the localization of both vehicles (with the same GNSS receivers and dead reckoning sensors) and the detection of the leader by the follower to do cooperative driving. The localization problemis fully distributed, to achieve this, the localization of the other vehicle is suppose to be transmitted via V2V communication. We supposed for simplification here that the communication is done without any delay and we used time stamped localization estimates of the two cars in a post-processing way. In reality, the communication could be done with 802.11p systems, like the Cohda, using CAM standard messages.

During the experiments, we supposed that every data was

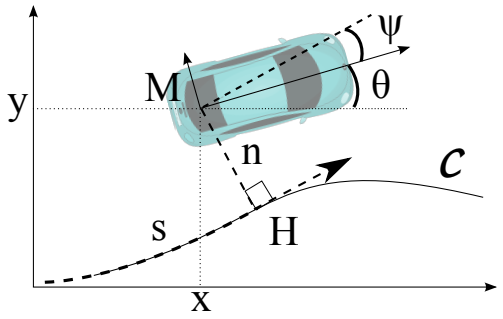

Fig. 3: Curvilinear coordinates.

synchronized and available at the same time. To solve sensor data asynchrony, we have done a linear interpolation of the data of the different sensors that were synchronized using GPS time.

III. Map

For autonomous driving, accurate georeferenced maps can give important information. Many works on this new maps are done to add new information, e.g. lane markings, road signs or environment around the road. These maps need to be very accurate to be used for autonomous driving. Indeed, vehicles use the center and the width of the road to stay in it.

The localization presented in this paper is intended for autonomous vehicles and use the center of the road as the reference.

The map used here has a few centimeter-accuracy and gives the center of the road with a set of points like open street map does. Originally, the map was build from clothoids. The set of points do not give all the pieces of information of the clothoids. For instance, curvature is missing.

IV. Curvilinear coordinates

A. Continuous map

To be closer to the reality, we chose to do the localization not in a classical Cartesian global frame where the pose is writen as $q_c = \begin{bmatrix} x & y & \theta \end{bmatrix}^T$but with curvilinear abscissa, curvilinear ordinate and curvilinear orientation leading to a curvilinear pose $q_s = \begin{bmatrix} s & n & \psi \end{bmatrix}^T$. This allows to know directly the pose of the vehicle relative to the road. These coordinates can be used directly for the control of an autonomous vehicle. The curvilinear abscissa can also give the along-track error which is computed with the arc-length from the start of the road and along the center of the road. The curvilinear ordinate can be used as the cross-track error from the center of the road. It is the orthogonal distance from the center of the road with a positive sign if the vehicle is on the left of the center of the oriented road and negative otherwise. The orientation of the vehicle relative to the road gives the angular error.

The first step, needed to convert a global pose into a curvilinear pose, is to do the map matching by finding the

closest point of the map from the position of the vehicle (point M in Fig. 3). This can be done by searching point H of the map that gives the orthogonal projection.

We can, after finding H, compute the arc length of the curve from the beginning of the road to point H. This arc length corresponds to the curvilinear abscissa. The distance MH gives the curvilinear ordinate. If point M is on the right of the tangent at point H, a negative sign must be add to this curvilinear ordinate. The orientation of the vehicle in the curvilinear coordinates is the relative orientation from the global pose to the tangent at point H.

B. Discretized map

The road is given by a map composed of points that represent the center of the road. A simple solution to obtain an easy-to-use continuous model of the center of the road is to use these points to build a polyline.

With a polyline, map-matching is done by searching the distance from point M to each segment. This distance can be the distance from the orthogonal projection as illustrated in Fig. 4 case 1. It happens in most cases, when point M is between the two orthogonal dashed lines of the start point p_i and the end point p_{i+1} of the segment. When point M is between the two orthogonal dashed lines of the second case, map matching is done with point $H = p_i$. When every distance from point M to each segment is computed, the smallest distance gives the map-matched segment.

Once the map-matching is done, the curvilinear coordinates are computed for both cases. For case 1, the curvilinear abscissa corresponds to the sum of the length of every segments before the map-matched segment added with distance p_iH. The curvilinear ordinate corresponds to distance MH with a negative sign if point M is on the right of the segment $[p_i\, p_{i+1}]$ w.r.t. the orientation of this segment. The orientation is the relative orientation from the orientation of the segment $[p_i\, p_{i+1}]$.

In case 2, the curvilinear abscissa is just the sum of the length of every segments before the map-matched segment. The curvilinear ordinate becomes the distance Mp_i with the negative sign if point M is on the right of the segment $[p_i\, p_{i+1}]$ w.r.t. the orientation of this segment like in case 1. The orientation is the same as in case 1; it is the relative orientation from the orientation of segment $[p_i\, p_{i+1}]$. The curvilinear coordinates of point M in case 2 are the same as the curvilinear coordinates of point M' which can be computed in case 1.

In case 2, we use the segment $[p_i\, p_{i+1}]$ to do the projection. This is only one possible choice among an infinity of possibilities. A discontinuity of the tangent at point p_i appears in this case. This discontinuity creates a stationary value of the curvilinear abscissa and a jump of the relative orientation. Indeed, point M and every point of the dashed curve in Fig. 4-b have the same curvilinear coordinates. When the vehicle is between two segments as in Fig. 4-c, if point M is bellow point p_i, the map-matching jumps from one segment to the next. Fig. 5 shows the stationary value of the curvilinear abscissa and the jump of this value.

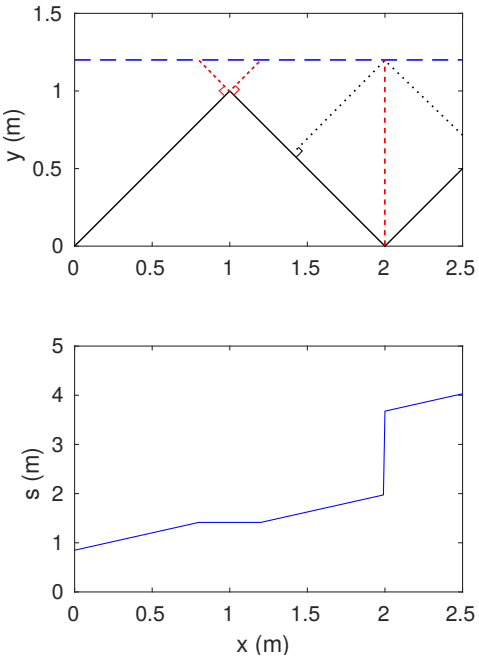

Fig. 5: Discontinuity issue of a discretized map.

The dashed blue line represents the path of the vehicle and the black polyline represents a discretized map with large discontinuity issues. One can see the curvilinear abscissa s (the blue curve) is constant between $x = 0.8$m and $x = 1.2$m and jumps when $x = 2$m.

In practice, when the angle between two following segments is very small, when the vehicle drives near the center of the road and when its position is sampled, the discontinuity does not appear. Point M does not stay in case 2 long enough if it goes in it, when the position is sampled.

To avoid this discontinuity, one can use the Lanelet transformation [1] or use a continuous and differentiable curve like a Hermite spline or a B-spline [13], [17].

V. One-dimensional cooperative data fusion

To be able to use their localization estimates to drive on roads, autonomous vehicles must have accurate values. The use of multiple sources of information gives the possibility to compute a more accurate localization but also to provide a better integrity.

In this work, the data fusion is done to provide an estimate of the curvilinear abscissa s. The curvilinear ordinate n and the curvilinear orientation ψ are supposed to be known.

A. Prediction

The first piece of information is the speed given by the wheel speed dead-reckoning sensors. This information is present in all cars and accessible through the CAN bus.

To obtain the curvilinear vehicle speed along the road in the polyline curvilinear coordinates, we project the speed of the vehicle into the closest segment. We use this speed to compute the prediction of the Kalman filter as follows:

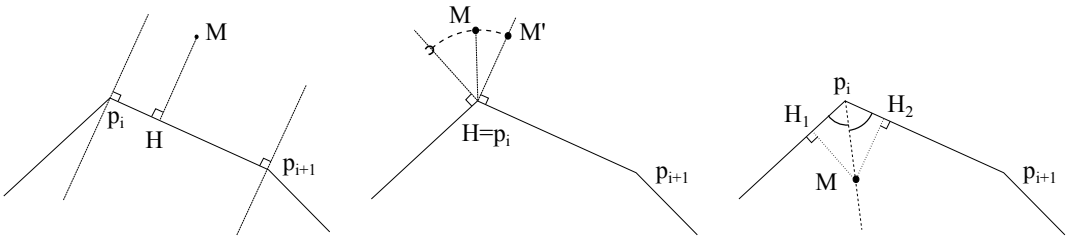

(a) case 1 (b) case 2 (c) case 3

Fig. 4: Discretized map.

$$\hat{s}_{k|k-1} = \hat{s}_{k-1|k-1} + T_e u_k \cos(\psi_{k-1}), \quad (1)$$

$$\hat{\sigma}^2_{s,k|k-1} = \hat{\sigma}^2_{s,k-1|k-1} + Q_{k-1}. \quad (2)$$

where σ represents the standard deviation of the curvilinear abscissa s, T_e is the sample time, Q_k is the variance of the prediction model and u_k is the longitudinal speed of the vehicle.

B. Kalman filter update

The second piece of information is the GNSS position given by the low cost mono-frequency GNSS receiver Ublox. This data is taken into account with a Kalman filter update. We note z_s the observation of the curvilinear abscissa with its standard deviation σ_{z_S}. The Kalman filter update follows the equations:

$$K_k = \hat{\sigma}^2_{s,k|k-1} / \left(\hat{\sigma}^2_{s,k|k-1} + \sigma^2_{z_s,k}\right), \quad (3)$$

$$\hat{s}_{k|k} = \hat{s}_{k|k-1} + K_k \left(z_{s,k} - \hat{s}_{k|k-1}\right), \quad (4)$$

$$\hat{\sigma}^2_{s,k|k} = \hat{\sigma}^2_{s,k|k-1} (1 - K_k)^2 + \sigma^2_{z_s,k} K_k. \quad (5)$$

Where K_k is the Kalman gain.

C. Covariance intersection filter update

The Kalman filter must be used with independent white errors. In the case where the errors fused are not independent, a phenomenon called *data incest* occurs and the result becomes overconfident.

To avoid this problem, a covariance intersection filter update can be used instead of the Kalman filter one. This filter is more pessimistic but remains consistent, i.e., the estimated variance is larger or equal to the true variance.

In one dimension, the covariance intersection filter can be written as follows:

$$\hat{\sigma}^2_{s,k|k} = (\omega/\hat{\sigma}^2_{s,k|k-1} + (1-\omega)/\sigma^2_{z_s,k})^{-1}, \quad (6)$$

$$\hat{s}_{k|k} = \hat{\sigma}^2_{s,k|k}(\omega \cdot \hat{s}_{k|k-1}/\hat{\sigma}^2_{s,k|k-1} + (1-\omega) \cdot z_{s,k}/\sigma^2_{z_s,k}). \quad (7)$$

where $\omega \in [0,1]$ is chosen so that $\hat{\sigma}^2_{s,k|k}$ is minimum. Minimizing $\hat{\sigma}^2_{s,k|k}$ is equivalent to maximizing

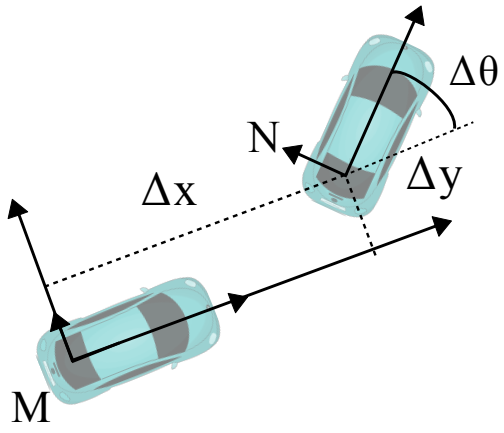

Fig. 6: Relative localization..

$$\omega \left(1/\hat{\sigma}^2_{s,k|k-1} - 1/\sigma^2_{z_s,k}\right) + 1/\sigma^2_{z_s,k}. \quad (8)$$

This is the equation of a line. So the maximum depends of the sign of $1/\hat{\sigma}^2_{s,k|k-1} - 1/\sigma^2_{z_s,k}$.

If $\hat{\sigma}^2_{s,k|k-1} < \sigma^2_{z_s,k}$, the maximum is reached for $\omega = 1$ and

$$\hat{s}_{k|k} = \hat{s}_{k|k-1}, \quad (9)$$

$$\hat{\sigma}^2_{s,k|k} = \hat{\sigma}^2_{s,k|k-1}. \quad (10)$$

Otherwise, if $\hat{\sigma}^2_{s,k|k-1} > \sigma^2_{z_s,k}$, the maximum is reached for $\omega = 0$ and

$$\hat{s}_{k|k} = z_{s,k}, \quad (11)$$

$$\hat{\sigma}^2_{s,k|k} = \sigma^2_{z_s,k}. \quad (12)$$

One can see that this one-dimensional covariance intersection is equivalent to keep only the estimator with the smallest variance.

D. Cooperative data fusion

The localization of the car is done thanks to a prediction using the speed of the car, then a Kalman filter update using the GNSS position. But it is possible to add an other Kalman update or a covariance intersection update when using V2V communication to receive the pose of an other vehicle. To be able to use this new information, the host vehicle must be

able to localize this other vehicle in its local frame. With this relative localization and the localization of the other vehicle, the pose of the host vehicle can be deduced.

Fig. 6 shows the relative pose ${}^{M}\Delta T_N = [\Delta x \Delta y \Delta\theta]$ that is needed in order to use the pose estimate of the other vehicle N to compute the pose of the host vehicle M:

$$\begin{aligned} q_c^M &= q_c^N - \begin{bmatrix} \cos(\theta^M) & -\sin(\theta^M) & 0 \\ \sin(\theta^M) & \cos(\theta^M) & 0 \\ 0 & 0 & 1 \end{bmatrix} {}^{M}\Delta T_N \quad (13) \\ &= \begin{bmatrix} x^N - \Delta x \cdot \cos(\theta^M) + \Delta y \cdot \sin(\theta^M) \\ y^N - \Delta x \cdot \sin(\theta^M) - \Delta y \cdot \cos(\theta^M) \\ \theta^N - \Delta\theta \end{bmatrix}. \end{aligned}$$

If we suppose that the curvilinear ordinate and the curvilinear orientation of the host and the other vehicle are known:

$$\Sigma_s^M = \begin{bmatrix} \sigma_s^{M2} & 0 & 0 \\ 0 & 0 & 0 \\ 0 & 0 & 0 \end{bmatrix}, \quad (14)$$

$$\Sigma_s^N = \begin{bmatrix} \sigma_s^{N2} & 0 & 0 \\ 0 & 0 & 0 \\ 0 & 0 & 0 \end{bmatrix}. \quad (15)$$

We can use the rotation matrix:

$${}^{M}R_N = \begin{bmatrix} \cos\Delta\alpha & -\sin\Delta\alpha & 0 \\ \sin\Delta\alpha & \cos\Delta\alpha & 0 \\ 0 & 0 & 0 \end{bmatrix}, \quad (16)$$

where $\Delta\alpha$ is the angle between the segment matched by the host vehicle and the segment matched by the other vehicle.

We can determinate the covariance matrix of the other vehicle Σ_s^N from the covariance matrix of the host vehicle Σ_s^M.

$$\begin{aligned} \Sigma_s^M &= {}^{M}R_N \cdot \Sigma_s^N \cdot {}^{M}R_N^{-1}, \quad (17) \\ &= \sigma_s^{N2} \begin{bmatrix} \cos^2\Delta\alpha & \cos\Delta\alpha \cdot \sin\Delta\alpha & 0 \\ \cos\Delta\alpha \cdot \sin\Delta\alpha & \sin^2\Delta\alpha & 0 \\ 0 & 0 & 0 \end{bmatrix}. \end{aligned}$$

By identification, we obtain:

$$\sigma_s^{M2} = \sigma_s^{N2}\cos^2(\Delta\alpha). \quad (18)$$

This new information with the relative localization and the global localization of the other car can be used to localize the host vehicle with a Kalman filter or a covariance intersection filter.

VI. Results

Fig. 7 and 8 present the error (blue curve) with the 5% confidence interval (red dashed curve) of the following and the leading vehicles using different sources of information fused with different methods (Kalman filter or covariance intersection filter). Graph A represents the error and the confidence interval of the curvilinear abscissa from the GNSS receiver used alone without any filter. Graph B shows

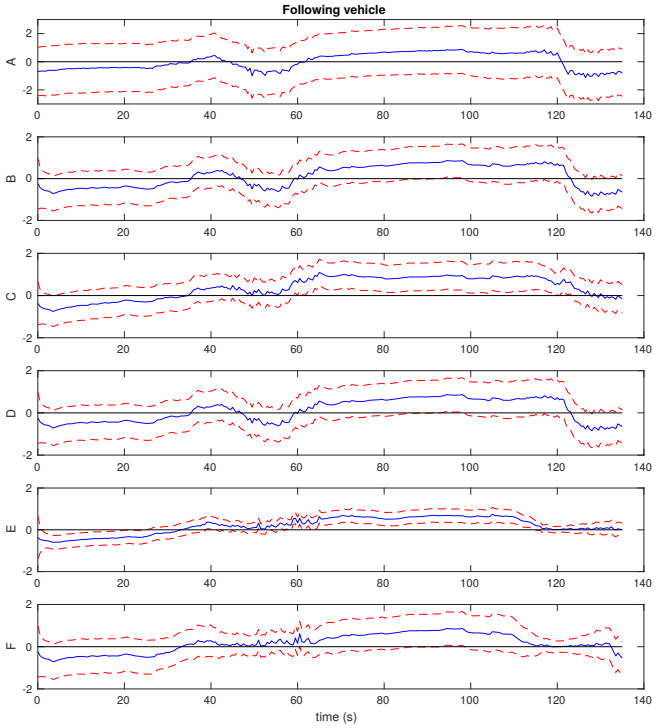

Fig. 7: Along-track errors (m) with 95% confidence intervals of the following vehicle.

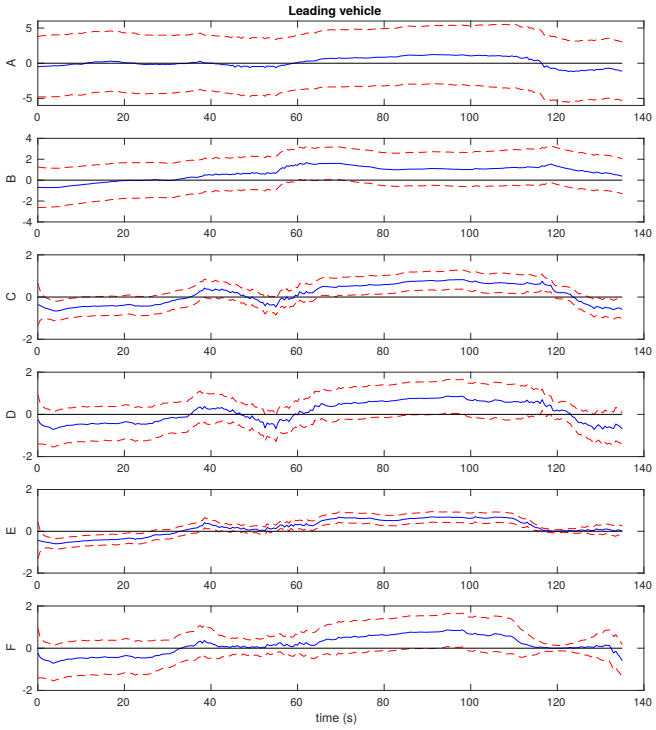

Fig. 8: Along-track errors (m) with 95% confidence intervals of the leading vehicle.

	Following vehicle		Leading vehicle	
	τ (%)	$\bar{e}$ (m)	τ (%)	$\bar{e}$ (m)
KF without communication (Fig. 7 and 8 B)	5.17	0.55	5.90	0.96
KF with communication from the leader to the follower (Fig. 7 C)	**47.60**	0.64 (+0.09)	5.90	0.96 (=)
CI with communication from the leader to the follower (Fig. 7 D)	5.17	0.55 (=)	5.90	0.96 (=)
KF with communication from the follower to the leader (Fig. 8 C)	5.17	0.55 (=)	**52.76**	0.50 (-0.46)
CI with communication from the follower to the leader (Fig. 8 D)	5.17	0.55 (=)	6.64	0.51(-0.45)
KF with bidirectional communication (Fig. 7 and 8 E)	**61.62**	0.44 (-0.11)	**69.00**	0.43 (-0.53)
CI with bidirectional communication (Fig. 7 and 8 F)	4.80	0.46 (-0.09)	4.43	0.45 (-0.51)

TABLE I: Experimental mean square errors and out-of-bound estimates.

the results obtained with a Kalman filter using the speed of the vehicle and the GNSS data. Graph C represents the case when the communication from the other vehicle (from the leader to the follower for the follower or from the follower to the leader for the leader) was added. Graph D corresponds to the same scenario as previously but by replacing the Kalman filter by the covariance intersection filter. Graph E shows the results when the communication was done in both direction while using a Kalman filter. Finally, Graph F is similar to the previous case but using the covariance intersection filter instead.

Tab. I shows the square root of the mean square error $\bar{e}$ and the rate of exceeding the 5% confidence interval τ for different sources of information fused with different methods.

The results in Tab. I show that when bidirectional communications are used with a Kalman filter, an over-convergence appears: the rate of exceeding the 5% confidence interval increased significantly. In contrast, when bidirectional communications are used with the covariance intersection filter, this rate decreases.

In these experiments, every time the communication is used with a Kalman filter, an over-convergence appears. Indeed, the errors of the GNSS receivers of the two cars were not independent because of the common mode errors (e.g. ionosphere delay or ephemeris errors). Another consequence resulting from this dependence is when a vehicle communicates a less accurate state estimate, the state of the second vehicle also becomes less accurate. This phenomenon can be seen in Tab. I. The following vehicle, which was more accurate than the leader, had its error increased when it used the communication with a Kalman filter. On the contrary, when the leader, which was less accurate, used the communication with a Kalman filter, its error decreased.

When communication is used, the covariance intersection filter must always be used to ensure the integrity of the error.

One can see that when one vehicle with an accurate GNSS receiver drives in a platoon of vehicles with less accurate GNSS receivers in the other cars, it can propagate its accuracy to the other vehicles.

According to Eq. 18 the accuracy increases when the difference of angle between the two map-matched segments (by the host vehicle and by the other vehicle) increases. This phenomenon can be seen in Fig. 7 and 8 around time 40s, 60s and time 115s, 130s when the vehicles were in the roundabout and when the bidirectional communication was used with a Kalman filter or a covariance intersection filter.

VII. Conclusion

This paper has presented a one-dimensional cooperative localization system using curvilinear abscissa along a reference map. We have focused on the along-track problem by supposing that the cross-track and heading errors are negligible. Real data from two Renault Zoé autonomous vehicles were used to obtain experimental results. The use of the covariance intersection filter instead of the Kalman filter when communication appear seems to be the best choice to avoid consistency issues. It has been also shown that the present algorithm for cooperative localization is very efficient to reduce the along-track error when the vehicles are driving on curved roads. Vehicles with accurate GNSS receivers can propagate their accurate localization to other vehicles. In a platoon, only one accurate vehicle localization can increase the localization of the whole platoon.

Acknowledgment: This work was carried out in the framework of Equipex ROBOTEX (ANR-10- EQPX-44-01) and Labex MS2T (ANR-11-IDEX-0004-02). It was also carried out within SIVALab, a shared laboratory between Renault, CNRS and UTC.

References

[1] P. Bender, J. Ziegler, and C. Stiller. Lanelets: Efficient map representation for autonomous driving. In *IEEE Intelligent Vehicles Symposium Proceedings*, pages 420–425, June 2014.

[2] L. C. Bento, Ph. Bonnifait, and U. J Nunes. Cooperative GNSS positioning aided by road-features measurements. *Transportation Research Part C: Emerging Technologies*, 79:42–57, 2017.

[3] D. Bétaille and R. Toledo-Moreo. Creating enhanced maps for lane-level vehicle navigation. *IEEE Transactions on Intelligent Transportation Systems*, 11(4):786–798, Dec 2010.

[4] K. Chu, M. Lee, and M. Sunwoo. Local path planning for off-road autonomous driving with avoidance of static obstacles. *IEEE Transactions on Intelligent Transportation Systems*, 13(4):1599–1616, December 2012.

[5] E. Héry, Ph. Xu, and Ph. Bonnifait. Along-track localization for cooperative autonomous vehicles. *IEEE Intelligent Vehicles Symposium*, June 2017.

[6] S. J. Julier and J. K. Uhlmann. A non-divergent estimation algorithm in the presence of unknown correlations. In *Proceedings of the American Control Conference*, volume 4, pages 2369–2373 vol.4, June 1997.

[7] N. Karam, F. Chausse, R. Aufrere, and R. Chapuis. Localization of a group of communicating vehicles by state exchange. In *IEEE/RSJ International Conference on Intelligent Robots and Systems*, pages 519–524, October 2006.

[8] J. Kim, K. Jo, W. Lim, M. Lee, and M. Sunwoo. Curvilinear-coordinate-based object and situation assessment for highly automated vehicles. *IEEE Transactions on Intelligent Transportation Systems*, 16(3):1559–1575, June 2015.

[9] F. Kuhnt, S. Orf, Sebastian Klemm, and J. M. Zöllner. Lane-precise localization of intelligent vehicles using the surrounding object constellation. In *IEEE 19th International Conference on Intelligent Transportation Systems*, pages 526–533, 2016.

[10] J. Levinson and S. Thrun. Robust vehicle localization in urban environments using probabilistic maps. In *IEEE International Conference on Robotics and Automation*, pages 4372–4378, 2010.

[11] H. Li and F. Nashashibi. Cooperative multi-vehicle localization using split covariance intersection filter. In *IEEE Intelligent Vehicles Symposium*, pages 211–216, June 2012.

[12] A. Martinelli, F. Pont, and R. Siegwart. Multi-robot localization using relative observations. In *IEEE International Conference on Robotics and Automation*, pages 2797–2802, April 2005.

[13] D. S. Meek and D. J. Walton. Planar G2 Hermite interpolation with some fair, C-shaped curves. *Journal of Computational and Applied Mathematics*, 139(1):141–161, February 2002.

[14] F. de Ponte Müller, E. M. Diaz, B. Kloiber, and T. Strang. Bayesian cooperative relative vehicle positioning using pseudorange differences. In *IEEE/ION Position, Location and Navigation Symposium*, pages 434–444, May 2014.

[15] M. Reinhardt, B. Noack, and U. D. Hanebeck. Closed-form optimization of covariance intersection for low-dimensional matrices. In *International Conference on Information Fusion*, pages 1891–1896, July 2012.

[16] Z. Tao, Ph. Bonnifait, V. Frémont, J. Ibanez Gusman, and S. Bonnet. Road-centred map-aided localization for driverless cars using single-frequency GNSS receivers. *Journal of Field Robotics*, June 2017.

[17] H. Wang, J. Kearney, and K. Atkinson. Arc-length parameterized spline curves for real-time simulation. In *Proc. 5th International Conference on Curves and Surfaces*, pages 387–396, 2002.